BIOCHEMISTRY
including biophysical chemistry & molecular biology

ARTICLE

pubs.acs.org/biochemistry

Highly Selective Ligand Binding by *Methylophilus methylotrophus* Cytochrome *c″*

Pedro O. Quintas,[†] Teresa Catarino,[†,‡] Smilja Todorovic,[†] and David L. Turner*[,†]

[†]Instituto de Tecnologia Química e Biológica, Universidade Nova de Lisboa, Av. da República, 2780-157 Oeiras, Portugal

[‡]Departamento de Química, Faculdade de Ciências e Tecnologia, FCT, Universidade Nova de Lisboa, 2829-516 Caparica, Portugal

Supporting Information

ABSTRACT: Cytochrome *c″* (cyt *c″*) from *Methylophilus methylotrophus* is unusual insofar as the heme has two axial histidine ligands in the oxidized form but one is detached when the protein is reduced. Despite cyt *c″* having an axial site available for binding small ligands, we show here that only NO binds readily to the ferrous cyt *c″*. Binding of CO, as well as CN^-, on the other hand requires considerable structural reorganization, or reduction of the disulfide bridge close to the heme. Standard free energies for the binding of NO and CO reveal high selectivity of the ferrous cyt *c″* for NO, indicating its putative physiological role. In this work, we characterize in detail the kinetics of NO binding and the structural features of the Fe^{2+}—NO adduct by stopped-flow and resonance Raman spectroscopy, respectively.

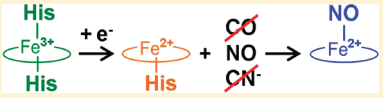

Binding of small gaseous diatomic molecules to heme proteins is of utmost importance for living cells. The heme group is indeed engineered to provide optimized binding of O_2, NO, and CO (i.e., XO), via effective back-donation of Fe(II) d_π electrons to low-lying π^* orbitals of these diatomic molecules.[1] Furthermore, heme proteins can fine-tune the Fe(II)—XO interaction to regulate signaling processes for diverse biochemical responses or undertake redox catalysis of these ligands. The mechanisms that allow heme proteins to discriminate between diatomic ligands are therefore of considerable interest. Examples include the oxygen transporters myoglobin and hemoglobin,[2−4] the oxygen sensor FixL,[5,6] the NO sensor guanylate cyclase,[7] and the CO sensor CooA.[8,9] Selectivity is thought to be achieved by regulating the relative binding affinities of the ligands through electrostatic interactions with the nearby amino acids and/or steric hindrance.[10]

Here we have investigated the ligand selectivity of cytochrome *c″* (cyt *c″*), a soluble monoheme protein isolated from the obligate aerobe *Methylophilus methylotrophus* that undergoes a redox-linked spin-state transition from low-spin (LS) in the oxidized form to high-spin (HS) in the reduced form[11] (see Figure 1). The axial ligands are two histidinyl residues with a near-perpendicular orientation in the oxidized form and a single proximal histidinyl residue in the reduced form (red5cc).[12] Previous work has also shown that reduction and alkylation of a disulfide bridge located near the heme led to a six-coordinate reduced form (red6cc), presumably with the previously detached histidine coordinated back to the heme iron.[13] So far, the physiological function of this cytochrome has not been determined; however, because of its ability to couple electron and proton transfer,[14] it has been suggested that it could serve as a model for more complex systems, such as cytochrome *c* oxidase.[15]

In this work, we address the ability of cyt *c″* to bind diatomic ligands. Typically, CO and O_2 bind to ferrous heme, because their π^* orbitals do not match the contracted $d\pi$ orbitals in ferric proteins.[1] NO is able to bind to both ferric and ferrous proteins, often forming only a transient adduct in the former case. In that respect, cyt *c″* is unusual because, despite the vacant distal axial position, it binds CO only upon major conformational rearrangement, caused by high temperature or pH, in the presence of high concentrations of urea, or upon reduction of the disulfide bond. Under these conditions, the protein undergoes a spin-state transition that results in a red6cc species (Figure 1) that binds CO and CN^- more readily. Moreover, ferrous cyt *c″* does not bind O_2, and the ferric protein does not bind NO. Nevertheless, NO is able to bind to ferrous cyt *c″* at physiological pH and temperature. To address the thermodynamic, kinetic, and structural features of the ferrous cyt *c″*—NO adduct, we performed binding, stopped-flow, and spectroscopic (resonance Raman) studies. Detailed comparison of standard free energies for the binding of NO and CO revealed the high selectivity of the ferrous cyt *c″* for NO, leading us to propose that it may be functionally relevant.

MATERIALS AND METHODS

Expression and Purification. The plasmid containing the cyt *c″* gene (pHS1)[16] was transformed into *Escherichia coli* strain BL21(DE3) harboring plasmid pEC86 encoding genes for cyt *c* maturation.[17] Where appropriate, antibiotics were added to a final concentration of 100 μg/mL (ampicillin) or 25 μg/mL (chloramphenicol). Cells were grown aerobically at 37 °C and 250 rpm in LB medium. For expression, IPTG was added to a concentration of 350 μM at a cell density (OD_{600}) of 3, and cells were harvested after 3−4 h by centrifugation (6500*g* for 20 min at 10 °C). Periplasmic fractions were isolated by osmotic shock, by resuspending the cells in 160 mL of 20% sucrose in 30 mM

Received: March 31, 2011
Revised: May 20, 2011
Published: May 21, 2011

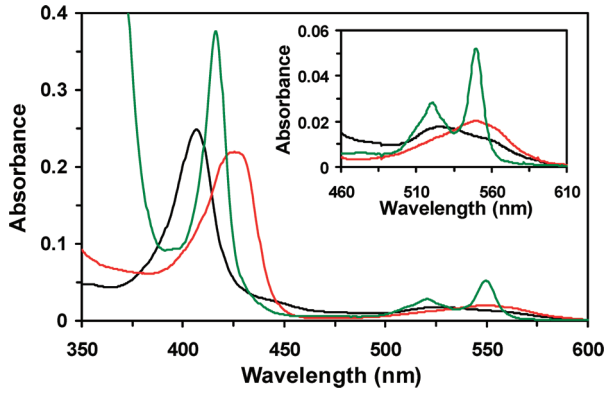

Figure 1. UV−visible spectra of oxidized (black), reduced five-coordinate (red), and reduced six-coordinate (green) cytochrome c''.[11,13] The reduced six-coordinate protein was obtained at pH 11.8 in the presence of 5 mM sodium dithionite.

Tris-HCl buffer (pH 7.5) containing 1 mM EDTA per liter of culture, followed by centrifugation (12500*g* for 20 min at 4 °C). The pellet was then resuspended in 60 mL of cold 5 mM $MgSO_4$, shaken for 10 min in an ice bath, and centrifuged under the same conditions. Cyt c'' was purified from the resulting supernatant by column chromatography in three steps: (i) ion exchange on a Q-Sepharose column (GE Healthcare) equilibrated with 5 mM Tris-HCl (pH 7.6) (cyt c'' does not adsorb to this column and elutes with the equilibrating buffer), (ii) ion exchange via application of the red fractions from step i to an S-Sepharose column (GE Healthcare) equilibrated with 5 mM Tris-HCl (pH 7.6) and elution with a salt gradient from 0 to 1 M NaCl prepared in the same buffer, and (iii) concentration of fractions containing cyt c'' by ultrafiltration (Amicon) and loading onto a Superdex-75 gel-filtration column (GE Healthcare) equilibrated with 100 mM potassium phosphate buffer (pH 7.5). The purification procedure was monitored by sodium dodecyl sulfate−polyacrylamide gel electrophoresis and UV−visible spectroscopy.

Binding of Small Molecules. The binding of nitric oxide (NO) was followed by optical absorption spectroscopy in a Shimadzu UV-1203 spectrophotometer placed inside an anaerobic chamber. Because it may react with the NO releasing compound or NO itself, care was taken to minimize the excess of sodium dithionite used to reduce cyt c''. The addition of NO was performed by injection of a small volume of a diethylamine NONOate solution in 10 mM NaOH with a gastight syringe ($[NONOate]_{final}$ = 50 μM). The protein sample was prepared in 100 mM phosphate buffer (pH 7.5). At this pH, each NONOate molecule releases 1.5 molecules of NO. The amount of NO present in solution at each time was obtained by studying the decay of the NONOate peak under the same conditions (ε_{250} = 6.5 mM^{-1} cm^{-1}).

The binding of carbon monoxide (CO) and cyanide (CN^-) was followed by optical absorption spectroscopy in a Shimadzu UV-1603 spectrophotometer connected to a thermostated bath, using a quartz optical cell with a path length of 10 mm, sealed with a silicone septum. Samples were prepared via injection of a few microliters of a concentrated protein solution into a degassed solution of the desired buffer. Reduction of the heme was achieved via addition of excess sodium dithionite solution with a gastight syringe. To reduce the disulfide bond, we added 5 mM dithiothreitol (DTT) to some samples. The addition of CN^- was performed via injection of a small volume of a potassium cyanide solution in the same buffer as the sample ($[CN^-]_{final}$ = 10 mM). The addition of CO was achieved by replacing argon in the headspace of the cuvette containing the protein sample with CO from a gas cylinder; this results in approximately 1 mM CO dissolved at 20 °C.[18] Binding of CO or CN^- was achieved by increasing the temperature of the sample in steps.

In each case, the amount of bound and unbound protein was determined by treating each spectrum as a weighted sum of the spectra of the two pure forms.

Effect of Temperature. The temperature was controlled by a circulating water bath connected to the spectrophotometer. Samples were prepared in degassed 100 mM phosphate buffer (pH 7.5). After the addition of the ligand, the temperature was increased until full binding was achieved (approximately 60 °C for CO and 70 °C for CN^-) and the temperature was quickly lowered by substitution of the hot water with room-temperature water. The effect of the temperature on the protein without any ligand was also studied using samples prepared in 100 mM phosphate buffer (pH 7.0) and 100 mM glycine-NaOH buffer at various pH values from 8.7 to 11.8.

Effect of Urea. Samples were prepared in degassed 100 mM phosphate buffer (pH 7) with various urea concentrations up to 6 M. The reversibility of the transition was studied by removing urea with a HiTrap desalting column (GE Healthcare). The effect of urea on the protein without any ligand was also studied using samples prepared in 100 mM phosphate buffer (pH 7.0) and 100 mM glycine-NaOH buffer at various pH values from 8.7 to 11.8.

Effect of DTT. In addition to binding experiments in the presence of DTT, protein samples treated with 5 mM DTT were titrated with reduced methyl viologen to determine the state of the disulfide bond. Untreated protein was titrated as a control, with 6 M urea as a denaturant in each case. A stock solution of methyl viologen was reduced by zinc under an anaerobic atmosphere, and its concentration was obtained from its UV−visible spectrum, using the value of absorbance at 605 nm and the extinction coefficient of 13.7 mM^{-1} cm^{-1}.[19] Aliquots (20 μL) were added to the protein sample, and then the UV−visible spectrum was recorded. The spectra recorded after each addition of methyl viologen were deconvoluted to obtain the contributions of the oxidized protein, the red5cc form, and the red6cc form, which are illustrated in Figure 1.

Kinetic Experiments. Stopped-flow kinetic experiments were performed at a constant temperature of 25 °C using a SF-61 DX2 stopped-flow apparatus (Hi-Tech Scientific) placed inside an anaerobic chamber (<2 ppm O_2). Solutions of reduced protein and NO were mixed, and the variation in absorbance in the UV−visible region was followed. The protein solution was prepared in the desired 100 mM phosphate buffer (pH 7.0) via addition of a small amount of a concentrated stock; NO solutions were prepared via addition of concentrated NONOate in 10 mM NaOH to the same buffer used for the protein in 1.8 mL flasks with no headspace. The solutions were then left for at least 1 h so that the NO was fully released, resulting in known NO concentrations in the range from 300 μM to 2.0 mM. We followed the reaction by either irradiating the sample with monochromatic light and measuring the absorbance at a single wavelength or irradiating the sample with light from a xenon lamp and detecting the transmitted light with a photodiode array (512 diodes, 280−700 nm range). All reactions were performed under pseudo-first-order conditions ([NO] ≫ [protein]), and traces were fitted with the sum of two exponentials. Second-order rate constants were obtained by

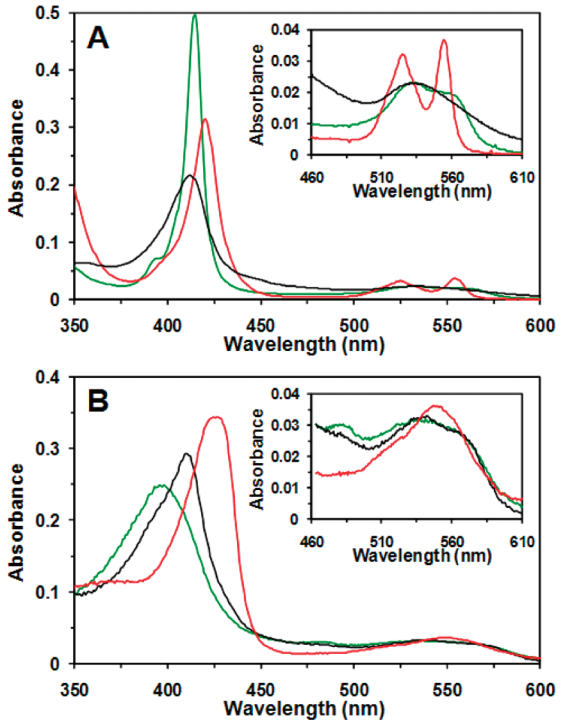

Figure 2. (A) UV−visible spectra of oxidized cyt *c″* bound to cyanide (black) and reduced cyt *c″* bound to cyanide (red) and carbon monoxide (green). (B) UV−visible spectra of reduced cyt *c″* in its native 5cc form (red) and reduced cyt *c″* bound to nitric oxide in the 6cc form (black) and 5cc form (green). The shoulder at ~400 nm in the spectrum of the 6cc form arises from imperfect deconvolution.

measuring pseudo-first-order rate constants as a function of NO concentration.

Resonance Raman Spectroscopy. All RR measurements were performed with a confocal microscope coupled to a Raman spectrometer (Jobin Yvon U1000) equipped with 1200 L/mm grating and a liquid nitrogen-cooled back-illuminated CCD detector. Samples were placed in a quartz rotating cell and excited with the 413 nm line from a krypton ion laser (Coherent Innova 302). Oxidized (as purified) and sodium dithionite-reduced cyt *c″* samples (100−200 μM) were measured at room temperature in the presence or absence of NO with a laser power of 8 mW and accumulation times of 60 s. The samples of reduced cyt *c″* in the presence of NO were prepared in an anaerobic chamber by the addition of excess NONOate to the cell filled with the protein solution in 10 mM Tris-HCl buffer (pH 7.6). UV−visible spectra were recorded after the Raman experiments to confirm the state of the sample.

After polynomial background subtraction, the positions and line widths of Raman bands were determined by component analysis in which the spectra of the individual species were fitted to the measured spectra using homemade software.

RESULTS

Binding of NO to Cyt *c″*. Binding of NO to ferrous cyt *c″* was followed via the characteristic blue shift of the Soret band (Figure 2 and Table 1), observed upon addition of small aliquots of NO-releasing diethylamine NONOate to dithionite-reduced protein. The UV−vis spectra were recorded, and in each case, the amount of NO-bound and free protein was determined by

Table 1. UV−Visible Spectroscopic Properties of Cyt *c″* and Its Adducts

	λ (nm) [ε (mM^{-1} cm^{-1})]			
	Soret	β	α	other
Fe^{3+} 6cc	407 (97.5)	526 (6.9)		
Fe^{2+} 5cc	426 (86.2)	550 (7.9)		
Fe^{2+} 6cc	416 (147.6)	521 (11.1)	550 (20.4)	
Fe^{2+}−NO 6cc	410 (73.6)	538 (8.1)		
Fe^{2+}−NO 5cc	398 (62.7)	535 (8.0)		482 (7.6)
Fe^{2+}−CO	415 (193.5)	532 (9.1)	563 (7.4)	
Fe^{2+}−CN^-	420 (123.7)	525 (12.7)	554 (14.5)	
Fe^{3+}−CN^-	412 (84.9)	534 (9.0)		

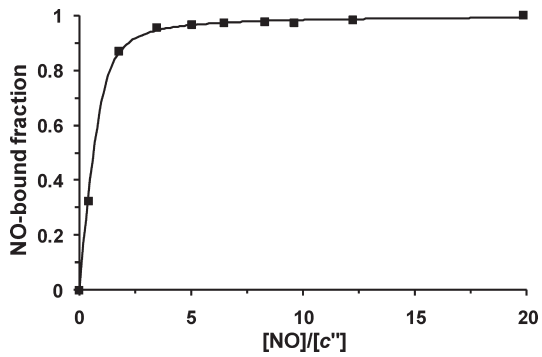

Figure 3. Binding of NO to reduced cyt *c″* (100 mM phosphate buffer, pH 7.5, 20 °C, [*c″*] = 2.5 μM). The NO-bound fraction accounts for the concentration ratio of NO-bound cyt *c″* to total cyt *c″*.

treating each spectrum as a weighted sum of the spectra of the two pure forms with electronic transitions at 398 and 426 nm.

At 20 °C and pH 7.5, NO binds to the reduced cyt *c″*, forming a 1:1 complex with a dissociation constant of 0.37 μM, which corresponds to a $\Delta G°$ for binding of −36.1 kJ/mol (see Figure 3). The UV−visible spectra in the presence of excess NO show no evidence of further reaction such as nitrosylation of the cysteines. Binding is fully reversible because removal of NO results in the UV−visible spectra of the ligand-free native HS state of ferrous cyt *c″*.

In the next step, stopped-flow experiments were conducted to study the kinetics of the reaction of reduced cyt *c″* with NO. An excess of ligand was used to ensure that the reaction occurred under pseudo-first-order conditions.

The reaction was followed by measuring the change in absorbance with time at 393, 407, and 426 nm, chosen by inspection of spectra obtained with the diode array, and corresponding to different contributions of the NO-bound five-coordinate (5cc), NO-bound six-coordinate (6cc), and red5cc forms. The time course traces show an increase in absorbance at 393 nm and a decrease at 426 nm, while at 407 nm, an increase is observed followed by a decrease (Figure 4). This suggests a mechanism in which NO binds to the reduced cyt *c″*, forming a 6cc NO−Fe−His intermediate, which is then converted to a 5cc NO−Fe form, with the detachment of the axial histidine. Each trace was fitted with a sum of two exponentials, as appropriate for consecutive reactions,[20] to obtain first-order rate constants k_1 and k_2 for NO binding and histidine detachment, respectively. Note that it is not necessary for the traces to represent pure forms

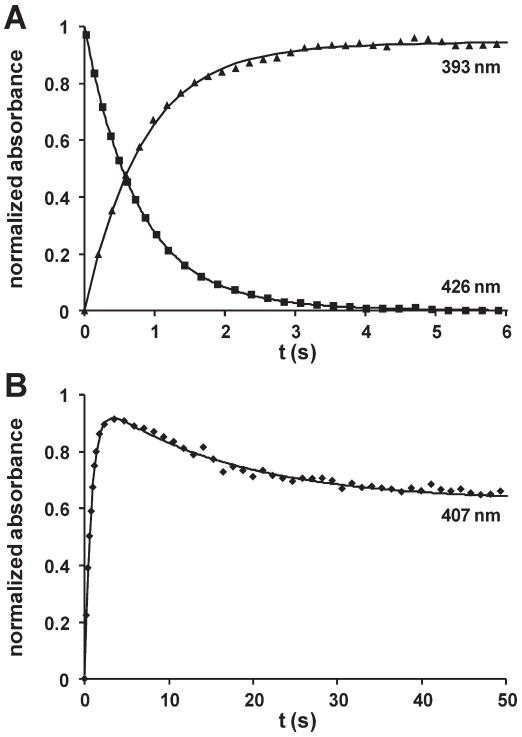

Figure 4. Time course traces at 393 and 426 nm (A) and 407 nm (B) for the reaction of 3 μM cyt c'' with 300 μM NO after mixing (100 mM phosphate buffer, pH 7.0, 25 °C). Solid lines represent the data fitted to the sum of two exponentials.

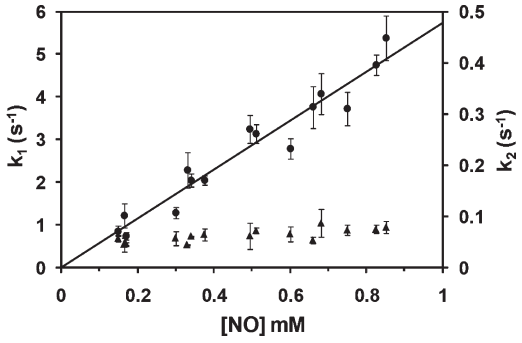

Figure 5. Dependence of k_1 (●) and k_2 (▲) on the concentration of NO. Values of k_1 and k_2 were obtained by fitting time course traces to a sum of two exponentials. Each point represents an average of separate fittings at different wavelengths, with the error bars representing twice the standard deviation.

to extract the rate constants; in fact, the wavelengths used here have contributions from more than one form. No change in the rates was observed when traces obtained at different wavelengths were used for the fitting.

The second-order rate constant for the binding of NO was determined from the slope of the straight line obtained by plotting the values of k_1 at different NO concentrations (Figure 5). The value obtained for k_{on} [$(5.7 \pm 0.2) \times 10^3$ M^{-1} s^{-1}] is lower than that determined for cytochrome c' (cyt c') and much lower than those for myoglobin and soluble guanylate cyclase (sGC) (Table 2).[21−23] The second process is clearly NO-independent, with a rate constant k_2 of 0.06 ± 0.01 s^{-1}, suggesting that NO does

Table 2. Rate Constants for the Binding of NO to Ferrous Hemoproteins

protein	temp (°C)	k_{on} (M^{-1} s^{-1})	ref
cyt c''	25	$(5.7 \pm 0.2) \times 10^3$	this work
cyt c'	25	4.4×10^4	21
Mb	20	1.7×10^7	22
sGC	15	$>1 \times 10^7$	23

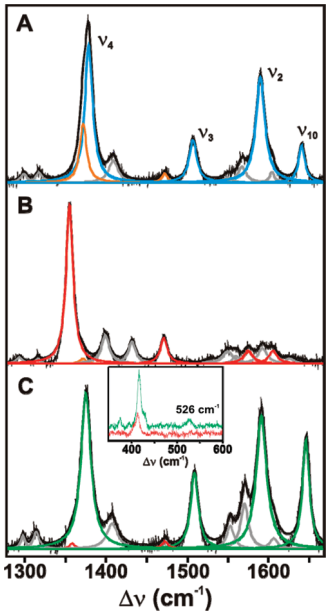

Figure 6. Experimental and component resonance Raman spectra of cyt c'' in the oxidized (A), reduced (B), and reduced NO-bound (C) forms, obtained with 413 nm excitation and 8 mW laser power. Marker bands are designated: oxidized 5cc (orange), oxidized 6cc (blue), reduced 5cc (red), and reduced NO-bound 5cc (green). The inset shows the low-frequency region of the NO-bound ferrous cyt c'' (top) and ferrous cyt c'' (bottom). Heme-state nonspecific traces are colored gray. Putative assignment of the bands is provided in the Supporting Information.

not bind to the proximal side of the heme, contrary to what was observed in the case of cyt c'.[21]

To understand the structural implications of NO binding, resonance Raman (RR) spectra of cyt c'' in the ferric, ferrous, and ferrous−NO adducts were measured. Vibrational modes ν_4, ν_3, ν_2, and ν_{10}, which appear in the high-frequency region (1300−1700 cm^{-1}) of the RR spectra, are sensitive marker bands of the spin, oxidation, and coordination state of the heme iron, allowing the identification and detailed characterization of the different states of cyt c''.

In the ferric state, the heme is mainly LS 6cc, as indicated by ν_4, ν_3, ν_2, and ν_{10} marker bands at 1378, 1507, 1590, and 1640 cm^{-1}, respectively (Figure 6A).[24] A minor contribution from a HS species, with ν_4 and ν_3 bands at 1371 and 1472 cm^{-1}, respectively, was also detected. It was present in all preparations and probably originates from cytochrome where one of the axial histidines detached from the heme.[24] In the ferrous state, only the red5cc form is present, with ν_4, ν_3, ν_2, and ν_{10} marker bands at 1355, 1471, 1575, and 1605 cm^{-1}, respectively (Figure 6B). The RR spectrum of the reduced protein shows strong similarities with

Table 3. Resonance Raman Frequencies for Five-Coordinate Nitrosyl Adducts

protein	ν_4 (cm^{-1})	ν_3 (cm^{-1})	ν_2 (cm^{-1})	ν_{10} (cm^{-1})	ref
cyt c''	1375	1508	1592	1647	this work
cyt c'	1373	1506	1592	1641	25
sGC	1375	1509	1584	1646	27
CooA	1376	1506	1582	1641	9

that of cyt c',[25] with downshifted ν_4 and unusually intense modes at 1400 and 1430 cm^{-1}. Upon reoxidation of the ferrous cyt c'', the two-population state of the oxidized form is fully re-established. In addition to out-of-plane porphyrin modes and deformation modes, an intense band at 228 cm^{-1} was detected in the low-frequency region (Figure S1 and Table S1 of the Supporting Information). We assign this mode to the Fe^{2+}—N(His) stretching coordinate that typically appears in the 190—250 cm^{-1} range; a relatively high frequency of this mode indicates H bonding interactions of the proximal His that bring about a partial imidazolate character.[26]

The RR spectrum of the ferrous NO-bound complex shows a population with ν_4, ν_3, ν_2, and ν_{10} modes at 1375, 1508, 1592, and 1647 cm^{-1}, respectively (Figure 6C). The values of the ν_4 frequencies are unusually high for a reduced heme because of the decrease in the electron density of the π^* antibonding orbitals of the porphyrin macrocycle by back-bonding to the NO through the iron d_π orbitals.[1] Similar frequencies were reported for NO adducts of ferrous CooA, sGC, and cyt c'[9,25,27] and attributed to a high-spin 5cc state, with NO bound to the heme and no proximal histidine ligand (Table 3).

Further evidence of the formation of a 5cc nitrosyl complex comes from the low-frequency region of the RR spectrum (300—600 cm^{-1}), where an additional broad band appears at 526 cm^{-1} in the presence of NO (Figure 6, inset, top trace). This band is clearly absent from the spectra of the ferrous protein (Figure 6, inset, bottom trace). The frequency of the band falls into the 520—526 cm^{-1} range observed in other 5cc NO adducts of *c*-type cytochromes and coincides with the Fe—NO stretching measured in the 5cc cyt c'—NO adduct.[25] The 6cc nitrosyl adducts of heme proteins, on the other hand, tend to have a stronger Fe^{2+}—NO bond, with the stretching frequency in the range of 536—576 cm^{-1}.[28]

In the UV—visible experiments, the final 5cc NO-bound product is only reached after >100 s. Kinetic experiments with detection by a photodiode array show a 5-fold increase in rate constant k_2, compared to the single-wavelength data obtained with the photomultiplier (data not shown). This cannot be an effect of temperature because the Arrhenius activation energies have been determined to be 57 ± 8 kJ/mol for k_1 and 171 ± 16 kJ/mol for k_2, but k_1 is not affected when the diode array is used. We attribute this effect to the fact that in kinetic experiments with the photodiode array, the sample is exposed to intense light, which may facilitate the detachment of the axial histidine. This was tested in the stopped-flow apparatus by switching on the light source after the reaction had proceeded for various times in the absence of light. In each case, the reaction proceeded normally and accelerated immediately when the light source was switched on.

Binding of CO and CN^- to Cyt c''. In the next step, we investigated the binding of other small ligands to cyt c'' by UV—visible spectroscopy. Under reducing conditions at 25 °C and pH 7.0, only ~10% of the protein binds CO, while under the same conditions, the binding of CN^- is negligible. Binding of CO and CN^- to the red5cc form is achieved only in the presence of urea or at increased temperatures. UV—visible spectra of the complexes of cyt c'' with CO and CN^- are shown in Figure 2, and the respective peak positions are listed in Table 1.

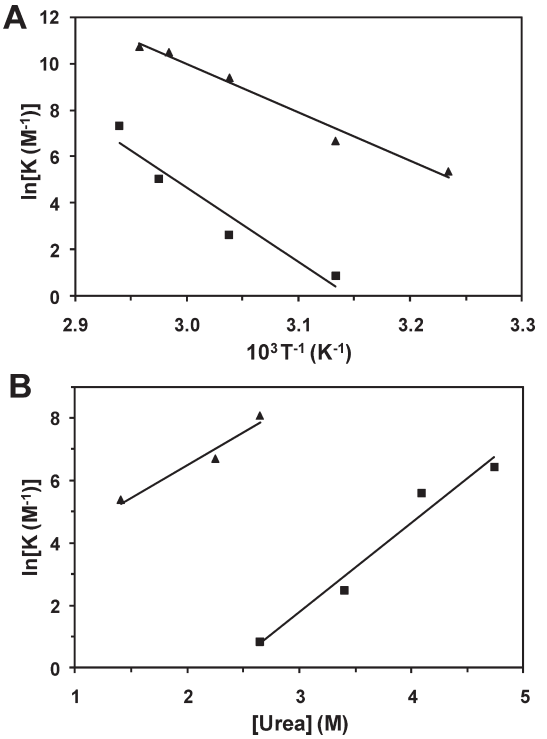

Figure 7. (A) Temperature dependence of the equilibrium constant of CO (▲) and CN^- (■) binding to reduced cyt c'' (100 mM phosphate buffer, pH 7.5, [CO] = 0.5—1 mM, [CN^-] = 10 mM, [c''] = 2.5 μM). (B) Variation of the equilibrium constant of CO (▲) and CN^- (■) binding to reduced cyt c'' with urea concentration (100 mM phosphate buffer, pH 7, 20 °C, [CO] = 1 mM, [CN^-] = 10 mM, [c''] = 2.5 μM).

Increasing the temperature results in an increase in the amount of the CO-bound form, with full binding achieved at ~60 °C. Lowering the temperature brings the protein back to its original, partially bound, state. Spectra were deconvoluted to obtain the bound (B) and unbound (U) fractions, and hence, the equilibrium constant K = [B]/([U][CO]) at each temperature (T). Plotting ln(K) versus $1/T$ (Figure 7A) and extrapolating to 293 K provided the value of $\Delta G°$ for the binding of CO at this temperature (Table 4).

Full binding of cyanide to ferrous cyt c'' can also be achieved by increasing the temperature to ~70 °C. Cyanide commonly binds to the iron in oxidized type *c* cytochromes, but CN^- binds fully to oxidized cyt c'' only at ~60 °C. In fact, the value found for $\Delta G°$ is similar to that for cyanide binding to the reduced form (Table 4). Lowering the temperature brings the protein back to the ligand-free form, in both cases. The binding of CO and CN^- to ferrous cyt c'' is fully reversible for most of the sample. The small fraction of bound protein present at the start of each experiment is slightly increased when the temperature is lowered at the end (~5% increase in the experiments with CO and 10% increase in the experiments with CN^-). This may be due to some irreversible denaturation of the protein at high temperatures that increases the affinity of the protein for the ligands. The effect is less

Table 4. Standard Free Energies of Binding and of the Reduced Five-Coordinate to Six-Coordinate Transition Obtained When either the Urea Concentration or the Temperature Was Varied[a]

	ΔG° (kJ/mol)			
	Fe^{2+}−CO binding	Fe^{2+}−CN^- binding	Fe^{3+}−CN^- binding	red5cc−red6cc transition
temperature	−3.5 ± 0.9	21 ± 2	16.9 ± 0.9	48 ± 4
urea	−6 ± 1	17 ± 2	6.6 ± 0.2	38 ± 2

[a] Values at 20 °C and pH 7 for urea and pH 7.5 for temperature.

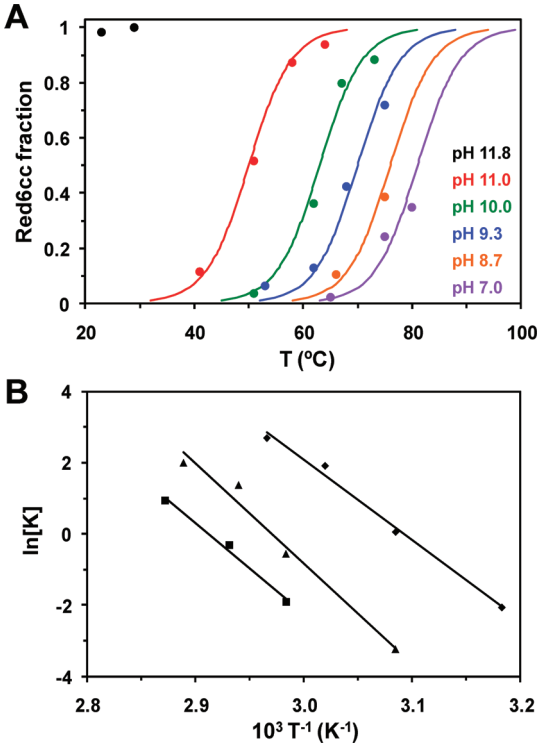

Figure 8. (A) Temperature dependence of the fraction of cyt *c*″ in the reduced six-coordinate form at different pH values in 100 mM glycine buffer except pH 7.0 in 100 mM phosphate buffer. The curves drawn are illustrative. (B) Variation of the equilibrium constant of the reduced five-coordinate to six-coordinate transition with temperature [100 mM glycine-NaOH buffer at pH 9.3 (■), 10.0 (▲), and 11.0 (◆)].

pronounced in the binding of CO, probably because the temperatures reached in these experiments were lower.

Similarly, high concentrations of urea (up to 6 M) facilitate the binding of both CO and CN^- to the reduced form of cyt *c*″. Approximate binding energies can be obtained by plotting ln(*K*) against the concentration of urea[29] (Figure 7B) and extrapolating to zero concentration (see Table 4). As in the case of elevated temperatures, the transition to the bound form is less favorable in the case of CN^- than in the case of CO. Removal of urea returns the protein to the reduced form with release of the ligand.

The binding of CN^- to the oxidized form is also favored by increasing the concentration of urea, but agreement with the ΔG° value obtained from the temperature dependence is worse than for the reduced form (Table 4).

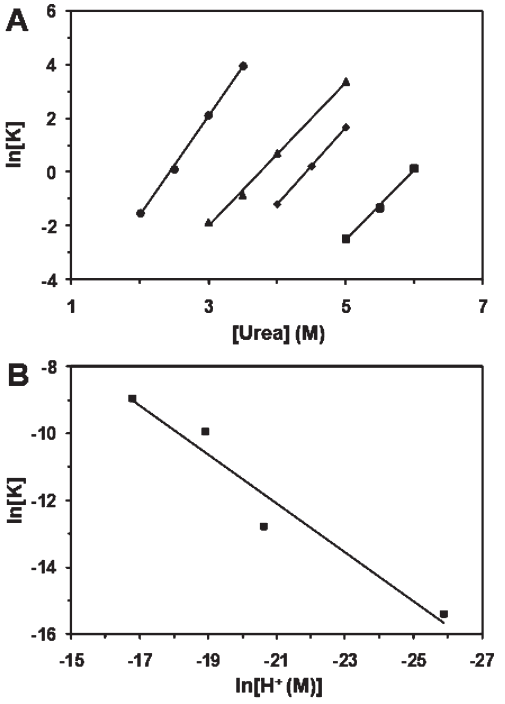

Figure 9. (A) Variation of the equilibrium constant of the reduced five-coordinate to six-coordinate transition with the concentration of urea, determined in 100 mM glycine-NaOH buffer at pH 11.0 (●), 10.0 (▲), and 9.3 (◆) and in 100 mM phosphate buffer at pH 7.0 (■). (B) pH dependence of the equilibrium constants obtained from panel A by extrapolation to zero urea.

Effect of Temperature in the Reduced Form. Increasing the temperature causes the UV−visible spectrum typical of the red5cc form to change to that of red6cc cyt *c*″ (see Figure 1) with a transition temperature that is pH-dependent, as shown in Figure 8A. At the highest pH value studied (11.8), the protein is already in the red6cc form at 23 °C, while at pH 7.0, only 35% of the protein is in this state at the highest temperature (80 °C). Assuming a two-state transition, we determined an equilibrium constant at 20 °C by extrapolation for each pH value (Figure 8B). A plot of ln(*K*) versus ln([H^+]) extrapolated to pH 7 then gave the value of ΔG° included in Table 4. Moreover, the slope of the plot gives the number of protons transferred in the process (1.5 ± 0.6).[30] We can rationalize the loss of one proton in the transition by formation of an imidazolate ion at high pH that may bind the iron more tightly than uncharged histidine. The change in conformation is almost fully reversible in this pH range, with only ~10% of the protein remaining in the red6cc form when the temperature is restored to ambient.

The UV−visible spectrum of the oxidized form does not change in the range of temperatures tested, although it should be noted that the ferric heme is already six-coordinate.

Effect of Urea in the Reduced Form. The UV−visible spectrum of the reduced HS cyt *c*″ also shows a conversion to the red6cc LS form with the addition of urea. The reversibility of the transition was proven by removal of urea by gel filtration, which brings the protein back to the native red5cc form. As demonstrated in the case of elevated temperature, high pH also facilitates the spin transition in the presence of urea. The ΔG° of the transition was calculated using the same procedures that were used previously (see Figure 9 and Table 4). The slope of the plot

Table 5. Standard Free Energies for the Binding of Nitric Oxide, Carbon Monoxide, and Cyanide to Different Heme Proteins

	$\Delta G°$ (kJ/mol)				
	Fe^{2+}−NO	Fe^{2+}−CO	Fe^{3+}−CN^-	Fe^{2+}−CN^-	ref
hemoglobin	−68 (R)/−56 (T)	−50 (R)/−34 (T)	−51	0	34−36
myoglobin	−63	−37	−41	−3	34, 37
cytochrome *c*	−31	–	−35	13	34, 38
cytochrome oxidase	−50	−37	−34	−19	34, 39
soluble guanylate cyclase	−67	−23	−17	–	34, 40, 41
cytochrome *c′*	−39	−17/−34	−11	–	42, 43
CooA	–	−35	–	–	44
cytochrome *c″*	−36	−4	17	21	this work

of $\ln(K)$ versus $\ln([H^+])$ is also compatible with the loss of one proton. As before, the UV−visible spectrum of the oxidized form does not change with urea in the absence of ligands. RR spectra further confirmed the formation of the red6cc species in urea-treated cyt *c″*, with ν_4 and ν_3 bands at 1360 and 1492 cm^{-1}, respectively (data not shown). Furthermore, as judged from the RR spectra in the presence or absence of urea, no structural alterations at the level of the heme cavity seem to occur in ferric cyt *c″*.

In view of the report that chemical modification of the disulfide bond near the heme produced a six-coordinate reduced cyt *c″*,[13] we sought to establish whether simple reduction of the disulfide would have the same effect. Treating the protein with DTT converted approximately half of the sample to the red6cc form, which binds both CO and CN^- readily. Because strong absorption by the heme in the UV−visible spectrum makes it impractical to use the Ellman assay, it was confirmed that the disulfide was reduced by titrating protein samples in 6 M urea with reduced methyl viologen. As a control, oxidized cyt *c″* was titrated with methyl viologen, which yielded red6cc, red5cc, and the ferric protein in a 6:4:1 ratio, determined by deconvolution of UV−visible spectra. Analysis of the titration curves showed that 1 equiv of methyl viologen is required to generate the red5cc protein, and a further 2 equiv is required to produce the red6cc form, as expected for reduction of the heme followed by reduction of the disulfide. Comparison with the data obtained in the titration of the sample treated with DTT showed that the red6cc produced in this way does not react further with methyl viologen. Thus, we conclude that the disulfide bridge is reduced in this form. The 5−10% of red6cc heme found in the reduced protein when restoring ambient temperature may therefore result from partial reduction of the disulfide by sodium dithionite.

DISCUSSION

Elucidating the binding properties of cyt *c″* proved to be difficult because of the unusual characteristics of this cytochrome. We show here that the stable five-coordinate form of reduced cyt *c″* reveals a high selectivity for NO, which is able to bind fully under physiological conditions. Other small ligands like CO and CN^- are able to bind to cyt *c″* only upon structural rearrangement. This conformational transition can take place under moderately denaturing conditions (high temperature, high pH, or high urea concentrations) or upon reduction of the disulfide bond, located in the vicinity of the heme. These denaturing conditions also promote reattachment of the distal histidine ligand in the reduced protein and accelerate the reduction of the disulfide by DTT.

According to the published structure of the reduced cyt *c″*,[31] the distance from the heme iron to the ring of the detached distal histidine is 5.6 Å, which is comparable with a distance of 6.1 Å between the iron and the ring of the detached proximal histidine in the NO complex of *Alcaligenes xylosoxidans* cyt *c′*.[32] Hence, steric hindrance is unlikely to be significant for NO when it is on the distal side of the heme in cyt *c″*, though the low rate constant for binding suggests that the entrance to the heme pocket may be hindered. A much lower affinity of the heme for CO might be a consequence of steric hindrance for a ligand that prefers to bind more nearly perpendicular to the heme. The distal histidine residue in cyt *c″* immediately precedes Cys96 of the disulfide bridge that braces a loop in the structure (Cys96−Cys104) and lends rigidity to that side of the heme pocket. The $\Delta G°$ values presented here do suggest that CO binding requires a significant conformational rearrangement of the protein. Therefore, by keeping the heme pocket tight, the presence of the disulfide plays a major role in the selectivity of the protein for NO. Although the selectivity of cyt *c″* is not at the level of sGC (see Table 5), it is greater than that observed in cyt *c′*, a small, soluble monoheme protein that has been associated with the capture and transfer of NO.[33] If the protein is brought into the "relaxed" form by a thermodynamically unfavorable structural rearrangement or partial denaturation, ligand binding is facilitated and the selectivity for NO binding is lost.

In *A. xylosoxidans* cyt *c′*, which is five-coordinate in both the oxidized and reduced forms, with histidine as the axial ligand, the crystal structures of the ferrous ligand-bound forms show that NO is bound to the proximal side of the heme, replacing the histidine, while CO binds to the distal side, with the histidine still attached on the proximal side.[32] A similar process is observed in the activation of sGC by NO, though it is not clear whether the active form has the NO bound to the proximal or distal side.[45,46] In ferrous cyt *c″*, the detachment of the proximal histidine is also verified, by both UV−visible and resonance Raman spectroscopies. The spectra show a high degree of similarity to other 5cc NO adducts, such as cyt *c′*, sGC, and CooA.[9,25,27,47] NO is able to displace the proximal ligand in cyt *c′* from *A. xylosoxidans* and *Rhodobacter sphaeroides*,[48] but no evidence of this was observed in cyt *c″*. The physiological role of cyt *c″* remains to be further investigated, including a possible role in transporting NO, but the high selectivity toward NO that we demonstrate in this work strongly suggests that NO binding is functionally relevant.

ASSOCIATED CONTENT

Supporting Information. One table of RR modes and one figure showing the low-frequency part of RR spectra of

cytochrome c''. This material is available free of charge via the Internet at http://pubs.acs.org.

AUTHOR INFORMATION

Corresponding Author

*Phone: (+351) 21 4469718. Fax: (+351) 21 4411277. E-mail: turner@itqb.unl.pt.

Funding Sources

This work was supported by PPCDT/QUI/58985/2004, PTDC/QUI/65640/2006, and Ph.D. Grant SFRH/BD/36716/2007 (to P.O.Q.).

ACKNOWLEDGMENT

We thank Isabel Pacheco and Patrícia Almeida for technical support and Helena Santos for support and advice.

ABBREVIATIONS

LS, low-spin; HS, high-spin; RR, resonance Raman; red5cc, reduced five-coordinate cytochrome c''; red6cc, reduced six-coordinate cytochrome c''; 5cc, five-coordinate; 6cc, six-coordinate.

REFERENCES

(1) Soldatova, A. V., Ibrahim, M., Olson, J. S., Czernuszewicz, R. S., and Spiro, T. G. (2010) New light on NO bonding in Fe(III) heme proteins from resonance Raman spectroscopy and DFT modeling. *J. Am. Chem. Soc. 132*, 4614–4625.

(2) Olson, J. S., and Phillips, G. N. (1997) Myoglobin discriminates between O_2, NO, and CO by electrostatic interactions with the bound ligand. *J. Biol. Inorg. Chem. 2*, 544–552.

(3) Springer, B. A., Sligar, S. G., Olson, J. S., and Phillips, G. N. (1994) Mechanisms of Ligand Recognition in Myoglobin. *Chem. Rev. 94*, 699–714.

(4) Baldwin, J. M. (1975) Structure and function of haemoglobin. *Prog. Biophys. Mol. Biol. 29*, 225–320.

(5) Gong, W., Hao, B., Mansy, S. S., Gonzalez, G., Gilles-Gonzalez, M. A., and Chan, M. K. (1998) Structure of a biological oxygen sensor: A new mechanism for heme-driven signal transduction. *Proc. Natl. Acad. Sci. U.S.A. 95*, 15177–15182.

(6) Gong, W., Hao, B., and Chan, M. K. (2000) New mechanistic insights from structural studies of the oxygen-sensing domain of *Bradyrhizobium japonicum* FixL. *Biochemistry 39*, 3955–3962.

(7) Zhao, Y., Brandish, P. E., Ballou, D. P., and Marletta, M. A. (1999) A molecular basis for nitric oxide sensing by soluble guanylate cyclase. *Proc. Natl. Acad. Sci. U.S.A. 96*, 14753–14758.

(8) Aono, S., Nakajima, H., Saito, K., and Okada, M. (1996) A novel heme protein that acts as a carbon monoxide-dependent transcriptional activator in *Rhodospirillum rubrum*. *Biochem. Biophys. Res. Commun. 228*, 752–756.

(9) Reynolds, M. F., Parks, R. B., Burstyn, J. N., Shelver, D., Thorsteinsson, M. V., Kerby, R. L., Roberts, G. P., Vogel, K. M., and Spiro, T. G. (2000) Electronic absorption, EPR, and resonance raman spectroscopy of CooA, a CO-sensing transcription activator from *R. rubrum*, reveals a five-coordinate NO-heme. *Biochemistry 39*, 388–396.

(10) Jain, R., and Chan, M. K. (2003) Mechanisms of ligand discrimination by heme proteins. *J. Biol. Inorg. Chem. 8*, 1–11.

(11) Santos, H., and Turner, D. L. (1988) Characterization and NMR studies of a novel cytochrome c isolated from *Methylophilus methylotrophus* which shows a redox-linked change of spin state. *Biochim. Biophys. Acta 954*, 277–286.

(12) Berry, M. J., George, S. J., Thomson, A. J., Santos, H., and Turner, D. L. (1990) Cytochrome c'' isolated from *Methylophilus methylotrophus*. An example of bis-histidine-co-ordinated Fe^{3+} haem, with near-perpendicular orientation of the ligands. *Biochem. J. 270*, 413–417.

(13) Brennan, L., Turner, D. L., Fareleira, P., and Santos, H. (2001) Solution structure of *Methylophilus methylotrophus* cytochrome c'': Insights into the structural basis of haem-ligand detachment. *J. Mol. Biol. 308*, 353–365.

(14) Costa, H. S., Santos, H., Turner, D. L., and Xavier, A. V. (1992) Involvement of a labile axial histidine in coupling electron and proton transfer in *Methylophilus methylotrophus* cytochrome c''. *Eur. J. Biochem. 208*, 427–433.

(15) Xavier, A. V. (2002) A mechano-chemical model for energy transduction in cytochrome *c* oxidase: The work of a Maxwell's god. *FEBS Lett. 532*, 261–266.

(16) Price, N. J., Brennan, L., Faria, T. Q., Vijgenboom, E., Canters, G. W., Turner, D. L., and Santos, H. (2000) High yield of *Methylophilus methylotrophus* cytochrome c'' by coexpression with cytochrome *c* maturation gene cluster from *Escherichia coli*. *Protein Expression Purif. 20*, 444–450.

(17) Arslan, E., Schulz, H., Zufferey, R., Kunzler, P., and Thony-Meyer, L. (1998) Overproduction of the *Bradyrhizobium japonicum* *c*-type cytochrome subunits of the cbb_3 oxidase in *Escherichia coli*. *Biochem. Biophys. Res. Commun. 251*, 744–747.

(18) Stephen, H., Stephen, T., and Kafarov, V. V. (1963) *Solubilities of inorganic and organic compounds*, Pergamon Press, Oxford, U.K.

(19) Watanabe, T., and Honda, K. (1982) Measurement of the Extinction Coefficient of the Methyl Viologen Cation Radical and the Efficiency of Its Formation by Semiconductor Photocatalysis. *J. Phys. Chem. 86*, 2617–2619.

(20) Catarino, T., and Turner, D. L. (2001) Thermodynamic control of electron transfer rates in multicentre redox proteins. *ChemBioChem 2*, 416–424.

(21) Andrew, C. R., George, S. J., Lawson, D. M., and Eady, R. R. (2002) Six- to five-coordinate heme-nitrosyl conversion in cytochrome c' and its relevance to guanylate cyclase. *Biochemistry 41*, 2353–2360.

(22) Moore, E. G., and Gibson, Q. H. (1976) Cooperativity in the dissociation of nitric oxide from hemoglobin. *J. Biol. Chem. 251*, 2788–2794.

(23) Makino, R., Matsuda, H., Obayashi, E., Shiro, Y., Iizuka, T., and Hori, H. (1999) EPR characterization of axial bond in metal center of native and cobalt-substituted guanylate cyclase. *J. Biol. Chem. 274*, 7714–7723.

(24) Rivas, L., Murgida, D. H., and Hildebrandt, P. (2001) Surface-enhanced resonance Raman study of cytochrome c'' from *Methylophilus methylotrophus*. *J. Mol. Struct. 565*, 193–196.

(25) Andrew, C. R., Green, E. L., Lawson, D. M., and Eady, R. R. (2001) Resonance Raman studies of cytochrome c' support the binding of NO and CO to opposite sides of the heme: implications for ligand discrimination in heme-based sensors. *Biochemistry 40*, 4115–4122.

(26) Othman, S., Richaud, P., Vermeglio, A., and Desbois, A. (1996) Evidence for a proximal histidine interaction in the structure of cytochromes *c* in solution: A resonance Raman study. *Biochemistry 35*, 9224–9234.

(27) Deinum, G., Stone, J. R., Babcock, G. T., and Marletta, M. A. (1996) Binding of nitric oxide and carbon monoxide to soluble guanylate cyclase as observed with Resonance raman spectroscopy. *Biochemistry 35*, 1540–1547.

(28) Lukat-Rodgers, G. S., and Rodgers, K. R. (1997) Characterization of ferrous FixL-nitric oxide adducts by resonance Raman spectroscopy. *Biochemistry 36*, 4178–4187.

(29) Makhatadze, G. I. (1999) Thermodynamics of protein interactions with urea and guanidinium hydrochloride. *J. Phys. Chem. B 103*, 4781–4785.

(30) Wyman, J., Jr. (1964) Linked Functions and Reciprocal Effects in Hemoglobin: A Second Look. *Adv. Protein Chem. 19*, 223–286.

(31) Enguita, F. J., Pohl, E., Turner, D. L., Santos, H., and Carrondo, M. A. (2006) Structural evidence for a proton transfer pathway coupled with haem reduction of cytochrome c'' from *Methylophilus methylotrophus*. *J. Biol. Inorg. Chem. 11*, 189–196.

(32) Lawson, D. M., Stevenson, C. E., Andrew, C. R., and Eady, R. R. (2000) Unprecedented proximal binding of nitric oxide to heme: Implications for guanylate cyclase. *EMBO J. 19*, 5661–5671.

(33) Moir, J. W. (1999) Cytochrome c' from *Paracoccus denitrificans*: Spectroscopic studies consistent with a role for the protein in nitric oxide metabolism. *Biochim. Biophys. Acta 1430*, 65–72.

(34) Cooper, C. E. (1999) Nitric oxide and iron proteins. *Biochim. Biophys. Acta 1411*, 290–309.

(35) Antonini, E., and Brunori, M. (1971) *Hemoglobin and myoglobin in their reactions with ligands*, North-Holland Publishing Co., Amsterdam.

(36) Cassoly, R., and Gibson, Q. (1975) Conformation, co-operativity and ligand binding in human hemoglobin. *J. Mol. Biol. 91*, 301–313.

(37) Cox, R. P., and Hollaway, M. R. (1977) The reduction by dithionite of Fe(III) myoglobin derivatives with different ligands attached to the iron atom. A study by rapid-wavelength-scanning stopped-flow spectrophotometry. *Eur. J. Biochem. 74*, 575–587.

(38) Schejter, A., Ryan, M. D., Blizzard, E. R., Zhang, C., Margoliash, E., and Feinberg, B. A. (2006) The redox couple of the cytochrome *c* cyanide complex: The contribution of heme iron ligation to the structural stability, chemical reactivity, and physiological behavior of horse cytochrome *c*. *Protein Sci. 15*, 234–241.

(39) Jones, M. G., Bickar, D., Wilson, M. T., Brunori, M., Colosimo, A., and Sarti, P. (1984) A re-examination of the reactions of cyanide with cytochrome *c* oxidase. *Biochem. J. 220*, 57–66.

(40) Stone, J. R., and Marletta, M. A. (1995) The ferrous heme of soluble guanylate cyclase: Formation of hexacoordinate complexes with carbon monoxide and nitrosomethane. *Biochemistry 34*, 16397–16403.

(41) Stone, J. R., Sands, R. H., Dunham, W. R., and Marletta, M. A. (1996) Spectral and ligand-binding properties of an unusual hemoprotein, the ferric form of soluble guanylate cyclase. *Biochemistry 35*, 3258–3262.

(42) Mayburd, A. L., and Kassner, R. J. (2002) Mechanism and biological role of nitric oxide binding to cytochrome c'. *Biochemistry 41*, 11582–11591.

(43) Kassner, R. J. (1991) Ligand binding properties of cytochromes c'. *Biochim. Biophys. Acta 1058*, 8–12.

(44) Kuchinskas, M., Li, H., Conrad, M., Roberts, G., and Poulos, T. L. (2006) The role of the DNA-binding domains in CooA activation. *Biochemistry 45*, 7148–7153.

(45) Russwurm, M., and Koesling, D. (2004) NO activation of guanylyl cyclase. *EMBO J. 23*, 4443–4450.

(46) Fernhoff, N. B., Derbyshire, E. R., and Marletta, M. A. (2009) A nitric oxide/cysteine interaction mediates the activation of soluble guanylate cyclase. *Proc. Natl. Acad. Sci. U.S.A. 106*, 21602–21607.

(47) Stone, J. R., and Marletta, M. A. (1994) Soluble guanylate cyclase from bovine lung: Activation with nitric oxide and carbon monoxide and spectral characterization of the ferrous and ferric states. *Biochemistry 33*, 5636–5640.

(48) Lee, B., Usov, O. M., Grigoryants, V. M., Myers, W. K., Shapleigh, J. P., and Scholes, C. P. (2009) The role of arginine-127 at the proximal NO-binding site in determining the electronic structure and function of 5-coordinate NO-heme in cytochrome c' of *Rhodobacter sphaeroides*. *Biochemistry 48*, 8985–8993.